A mica/nepheline glass-ceramic prepared by melting and powder metallurgy at low temperatures

Wei, Wei; Yong, Liu; Yanni, Tan; Grover, Liam; Yu, Guo; Bowei, Liu

DOI:
10.1016/j.mtcomm.2017.02.007

Title: A mica/nepheline glass-ceramic prepared by melting and powder metallurgy at low temperatures

Authors: Wei wei, Liu Yong, Tan Yanni, Liam Grover, Guo Yu, Liu Bowei

PII: S2352-4928(16)30133-7
DOI: http://dx.doi.org/doi:10.1016/j.mtcomm.2017.02.007
Reference: MTCOMM 159

To appear in:

Received date: 2-11-2016
Accepted date: 3-2-2017

Please cite this article as: Wei wei, Liu Yong, Tan Yanni, Liam Grover, Guo Yu, Liu Bowei, A mica/nepheline glass-ceramic prepared by melting and powder metallurgy at low temperatures, Materials Today Communications http://dx.doi.org/10.1016/j.mtcomm.2017.02.007

A mica/nepheline glass-ceramic prepared by melting and powder metallurgy at low temperatures

Wei wei [a], Liu Yong [a,*], Tan Yanni [a,*], Liam Grover [b], Guo Yu [a], Liu Bowei [a]

[a]State Key Laboratory of Powder Metallurgy, Central South University, Changsha 410083, PR China

[b]School of Chemical Engineering, University of Birmingham, Edgbaston, Birmingham, B15 2TT, UK

*Corresponding Author, Liu Yong, e-mail: yonliu@csu.edu.cn;

Tan Yanni, e-mail: tanyanni@csu.edu.cn

Graphical Abstract

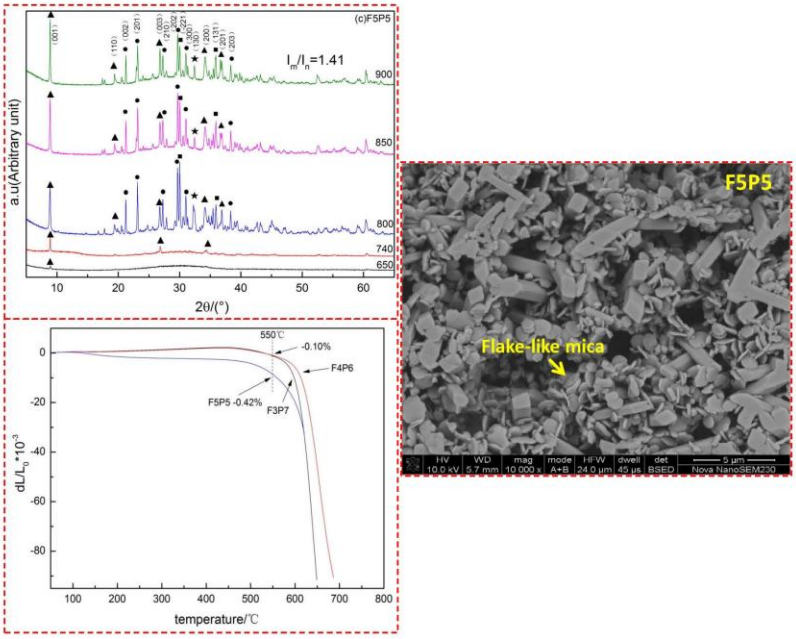

Highlights

1. Mica glass ceramics were prepared at low temperatures by melting and powder metallurgy.
2. The relative sintered density of mica glass ceramics at 850 °C can be 90%.
3. The microstructures of sintered glass ceramics are well crystallized, with mica and nepheline as main phases.
4. The transverse rupture strength and the hardness of mica glass ceramics can be 97 MPa and 6 GPa, respectively.

Abstract:

Mica glass-ceramics usually have high melting temperatures. In this work, mica glass-ceramics were prepared by the combination of melting and powder metallurgy at low temperatures. Firstly, a SiO_2-CaO-B_2O_3-MgO-Na_2O-ZnO glass powder with a melting temperature as low as 1000 °C was prepared. Subsequently, the glass powder mixed with different contents of fluorphlogopite was remelted at 1300 °C to synthesize the ultimate glass frit. After disintegration, the mica glass-ceramic powder can be sintered at low temperatures of 800-950 °C, and a relative density as high as 90% can be obtained. The phase constitutions and microstructures of the bulk glass-ceramics were characterized by X-ray diffraction and scanning electron microscopy. The results illustrated that the glass-ceramics were mainly made up of flake-like fluormica and columnar nepheline, accompanied by augite, forsterite and some other minor phases. The transverse rupture strength and the hardness of mica glass-ceramics were both low at 800℃ for the high porosity, and decreased with the increase of mica phase at 850 ℃. Nevertheless, the highest strength of the glass-ceramic with 30% mica reached 97.42±10.2 MPa, which can be potentially applied for engineering applications.

Keywords: glass-ceramic; mica; mechanical property; powder metallurgy

1. Introduction

Glass-ceramics are a kind of new material formed through the controlled nucleation and crystallization of glass, which combine the advantages of glass and ceramics. In the 1970s, Beall developed mica glass-ceramics, which were well-known for the good machinability because of the cleavage along (001) plane [1-3]. Since the development, mica glass-ceramics have had wide applications in aviation, biological implants, and electrical insulation [4-6]. These kinds of mica glass-ceramics were also successfully

commercialized as Macor® and Bioverit® [7, 8].

There are mainly three ways to fabricate mica glass-ceramics, such as casting, sintering, and sol-gel method [9]. Compared with casting and sol-gel method, sintering method is more convenient and cost-saving for preparing some glass-ceramics, especially for some materials with refractory oxides or complex phases. Usually, glass-ceramics should be melted one or two times, and then crystallize through annealing or sintering processes. However, if the parent glass is melted according to the chemical composition of $KMg_3(AlSi_3O_{10})F_2$, fluorphlogopite phases can not be obtained by annealing[10]. By adding B_2O_3 and increasing the content of SiO_2 and Al_2O_3, Corning developed stable mica glass-ceramics[11]. But, the melting temperature of mica glass-ceramics is always high, which makes high requirement on industrial equipment and increases energy consumption. Therefore, much effort has been paid to lower the melting temperature of mica glass-ceramics, including the additions of K_2O, Na_2O, B_2O_3, Li_2O, ZnO and other glass structure modifiers[12]. Qin[13] found that after adding 9 wt% ZnO to SiO_2-MgO-Al_2O_3-K_2O-CaO-P_2O_5-F system, the melting temperature of the bioactive glass-ceramics can be reduced to 1300 °C. Ma[14] lowered the melting temperature of the mica glass to 1200 °C by adding 3~7 wt% Li_2O, and 2~12 wt% ZnO. Wei[15] also lowered the melting temperature of mica glass to 1240 °C with the help of B_2O_3, Li_2O and ZnO. Besides, it is reported that 30-60 vol% amorphous fluorphlogopite can be formed by calcining kaolin and fluoride, with B_2O_3 as sintering aids, at about 1100 °C, without the melting step[16].

In this work, a kind of parent glass powder, which contained 24 wt% B_2O_3, 7 wt% ZnO and 7 wt% Na_2O[17], with a low melting temperature of 1000 °C was prepared firstly. Then, 30-50 wt% pure fluorphlogopite were melted with the parent glass to form new compositions. Finally, the glass-ceramic powder was sintered both for the densification and the crystallization. The microstructures and mechanical properties

were investigated.

2. Materials and Methods

2.1 Materials preparation

The parent glass was prepared from reagent grade chemicals. The compositions of the parent glass are displayed in Table 1. Firstly, the chemicals were fully blended and melted in a corundum crucible at 1000 °C for 2h in an electric furnace. The molten glass was quenched in cold water and pulverized. Then, the parent glass powder was mixed homogeneously with fluorphlogopite powder in different proportions (Table 2) (Hua Shuo Mineral Processing Co. Ltd. China), and heated at 1300 °C for 2h. After quenching, the new glass was well ground by ball milling in a corundum jar with alcohol as media for 24h. The dried powder was screened, and the particle size of three samples was measured with a MICRO-PLUS equipment to be between 5.8 to 6.4 μm.

The glass powder was mixed with 2.5 wt.% PVA, and cold pressed into 32×15×9 mm^3 bars at a pressure of 100 MPa on a laboratory uniaxial hydraulic press. Thereafter, the samples were heated at 550 °C to decompose binder, and sintered at 800, 850 or 900 °C with a heating rate of 5 °C /min.

2.2 Characterizations

2.2.1. Differential scanning calorimetry (DSC) and Dilatometry

Differential scanning calorimetry was done with a SDT Q600 thermal analyzer against α−alumina powder as the reference material. Nonisothermal experiments were performed by heating three kinds of sample powders, which would crystallize at different temperatures, at a heating rate of 5, 10, 15 and 20 °C/min, in the temperature range from ambient to 1000 °C.

After the decomposition of the binder, the compacts were cut into rectangular samples ($5\times5\times25$ mm^3). The sintering shrinkage behavior was investigated using a dilatometer (DIL 402 C, NETZSCH, Germany) at a heating rate of 5 °C /min in Ar atmosphere.

2.2.2. X-ray powder diffraction (XRD)

Identification of phases in the glass-ceramics was performed using X-ray powder diffraction equipment (SIMENS D500) with Cu target and Ni filter from 5° to 65°. The scanning speed was 2° (2θ) per minute with the step-length of 0.02° per step, and the accelerated voltage was 40 kV.

2.2.3. Scanning electron microscopy (SEM)

The microstructures of the gold coated samples were observed by SEM (Quanta FEG 250). Before sputtering, the glass-ceramics were polished, and thereafter chemically etched with 10% HF solution for 70 s. Besides, the sections after mechanical tests were also observed.

2.2.4. Mechanical properties

The mechanical properties of the glass-ceramics were studied by the three point bending method. More than 5 polished rectangular bars with dimension of $25\times12\times7$ mm^3 were used for each condition. A Vickers hardness tester with a diamond pyramid was utilized to measure hardness. The load was 200 g, and the loading time was 30 s. At least 10 indentations were made to obtain an average value of each specimen.

2.2.5. Density

The bulk density of the sintered samples was measured by the Archimedes method. The porosity of the samples was quantitatively measured through the images under an optical microscope by the software Image-Pro Plus.

3. Results and Discussion

3.1. Sintering behavior and crystallization

The XRD patterns of the three kinds of glass (F3P7, F4P6 and F5P5) are shown in Fig.1. It indicates that all the compositions are amorphous in nature after quenching. DSC curves of the three compositions are shown in Fig.2, and the characteristic temperatures are summarized in Table 3. Apparently, there are two main wide exothermic peaks (T_{p1} and T_{p2}) appearing in all samples. Based on the table, it is obvious that with the increasing heating rate, the glass transition temperature (T_g) and the crystallization temperature (T_{p1} and T_{p2}) increase, and the temperature range of densification $\Delta T=Tp_1-T_g$ is also improved. It is supposed that mica improves the sintering ability of the glass powders from F3P7 to F4P6 because it shifts the crystallization process to higher temperatures and broadens ΔT. Usually, the larger the difference ΔT is, the better stability of the glass against crystallization, and the easier the sintering of glass compacts will be from T_g to T_{p1}, because the larger ΔT can provide more heating time at a fixed heating rate.

The dimensional change of the compact bars during heating, indicating the sintering shrinkage behavior, is displayed in Fig.3. There are few differences in sample dimensions from room temperature to 500 °C. At 550 °C, the shrinkage of F3P7 and F4P6 is about 0.10%，lower than that of F5P5(0.42%), which corresponds to the lower T_g of F5P5. From 600 to 662 °C (T_{p1} of F3P7), the curve drops dramatically, representing the beginning of intense densification.

The sintering process of glass powder is dependent on the viscous flow, which is closely related to temperature and powder size. To accomplish the densification, the glass compacts should finish sintering procedure before T_{p1}. When the temperature is higher than T_g, the surface energy works as driving force and the glass powder starts forming sintering neck, removing the gas and decreasing the pores. The smaller the glass grain is, the stronger the driving force is. Heating at a temperature higher than T_{p1} causes the start of the nucleation and crystal growth. However, the new crystal

will increase the viscosity and inhibit the sintering. The densification results at different temperatures are shown in Table 4. It can be seen that at 800 °C, the porosity is higher than 15% and it decreases at 850 or 900 °C. However the porosity is still high slightly, because there is no holding time around T_{p1}, and the sintering time is too short. On the other hand, it is not until T_{p1} that the glass starts to crystallize really. During the sintering, the surface impurity and deficiency will induce the nucleation and growth below T_{p1}.

When the temperature reaches the crystallization point in DSC, the nucleation appears around the interface of sintered grains largely. The glass in the study is easy to crystallize at low temperatures. Firstly, the glass stability is weak, because the content of glass network modifiers (K^+, Na^+, Mg^{2+}, Ca^{2+}, Zn^{2+}) is high, which leads to the molar ratio of O to network formers (Si, B, Al) between 2:1 and 3:1. Secondly, some glass network modifiers have stronger field strength than alkali metal ion. Zinc oxide is a useful constituent for forming crystals in glass-ceramics because the field strength of the Zn^{2+} (z/a^2=0.52-0.59) is fairly higher than Ca^{2+} (z/a^2=0.33-0.35) and Mg^{2+} (z/a^2=0.45-0.51)[18], and it will form ordered structure with surrounding O atoms more easily.

According to the XRD results in Fig.4, for F3P7, the diffraction peaks at 600 °C represent Al_2O_3, which comes from the corundum jar when crushing, and the peaks are overlapped at higher temperatures. The nepheline and mica peaks appear at 700 °C and 800 °C, which means that the T_{p1} and T_{p2} represent the crystallization of nepheline and mica, respectively. The condition of F4P6 is similar to F3P7. Differently, for F5P5, the sequence of crystallization is reversed, and the T_{p1} stands for mica.

Using the following modified form of Kissinger equation established by Matusita and Saka[19], the activation energy (E) is calculated and shown in Table 3:

$$ln\frac{T_p^2}{\beta} = \frac{E}{RT_p} + C \quad (5)$$

where β is the heating rate, R is the universal gas constant and C is constant.

The activation energy for the mica crystal growth of F3P7, F4P6 and F5P5 are 133±3.3 kJ/mol, 144.3±9.2 kJ/mol and 176.3±12.5 kJ/mol, respectively, which are lower than the value obtained by Cheng[20] (275±6 kJ/mol). The discrepancy may attribute to the difference in the chemical compositions. It also indicates that the activation energy of mica phase increases with the addition of the mica. For F3P7 and F4P6, the crystallization temperature of K-fluorphlogopite is higher than that in other studies(713 ± 2°C)[21], because the precipitation of nepheline will hinder the formation of mica crystal in the matrix. With the addition of fluorphlogopite (F5P5), the mica appears before nepheline.

Fig.4 shows the XRD patterns of the sintered samples from 600 °C to 900 °C. At 800 °C, some phases, like mica ($KMg_3(AlSi_3O_{10})F_2$), nepheline ($KNa_3Al_4Si_4O_{16}$), forsterite (Mg_2SiO_4), and augite ($Ca(Mg_{0.7}Al_{0.3})(Si_{1.7}Al_{0.3})O_6$) will exist. When the temperature is higher, the minor phase, cordierite ($Mg_2Al_4Si_5O_{18}$) becomes less and even disappears. However, mica and nepheline are the main phases in all the glass-ceramics above 800 °C. The results are in accordance with those in references[22, 23]. Through the comparison of the characteristic peak height ($I_{mica}/I_{nepheline}$) of mica and nepheline, the mica is increasing while the nepheline is decreasing from F3P7 to F5P5 clearly. Al atoms coming from the dissolution of those minor phases would combine with Si atoms to form [$AlSi_3O_{10}$], the net unit of mica, leading to the increase of mica.

3.2. Microstructures

The microstructures of the sintered specimens are shown in Fig.5 and Fig.6. As can be seen, an interlocking structure of flake-like mica crystals appears. In fact, the shapes of mica are varied, which are depending on the nucleation and the growth mechanism.

According to other studies, the crystal growth indexes *n* (*n* is the Avrami index) of mica are 3 and 4[24, 25], which indicates that mica crystals grow along two and three dimensions respectively. Holand and Vogel have attributed the flake-like morphology to the substitution of Mg^{2+} by Al^{3+} in the octahedral positions of the mica structure[7, 26].

At 800 °C, there are a few flake-like crystals dispersed in the matrix (Fig.5a, 5c and Fig.6a), while at 850 or 900 °C, the mica crystals grow obviously (Fig.5b, 5d, Fig.6b and Fig.6c), accompanied by the decreasing of the aspect ratio. The change of the aspect ratio of mica is listed in Table 4, which may promote the machinability. Except for the flake-like mica phase, there are some other columnar and acicular crystals. The columnar crystals are nepheline[27], and the acicular crystals are the lateral view of the flake-like mica, which can be seen more clearly under a high magnification in the upper right corner of Fig.6a.

3.3. Mechanical properties

Table 4 indicates the mechanical properties of the glass-ceramics. The transverse rupture strength decreases from 93.02 MPa (F3P7) to 78.02 MPa (F5P5) and the hardness decreases from 6.24 GPa (F3P7) to 4.03 GPa (F5P5) at 850 °C with the addition of mica phase. The transverse rupture strength and the hardness are influenced by many factors, like porosity, phases and the content of mica[11]. The porosity at 800 °C is higher than 20%, so both the strength and the hardness are extremely low. When the sintering temperature increases to 850 and 900 °C, the porosity decreases to about 10%, and the strength and the hardness increase apparently. For F3P7 and F5P5 sintered at 850 °C, the mechanical properties decrease mainly because of the changes of phase constitution. According to the results of $I_{mica}/I_{nepheline}$ in F3P7 and F5P5, the mica phase increases, accompanied by the decrease of nepheline phase. The strength and the hardness of nepheline glass-ceramics are about 120 ± 13 MPa and 6.6 ± 0.3 GPa, respectively[28], which are

higher than that of mica.

Based on the previous study, the flake-like mica phase has a tendency of plastic flow/deformation under loading[29], so the glass-ceramic containing a large amount of mica crystal (F5P5) has the lowest hardness. The interlocking structure in the glass-ceramic also helps in stopping the cracks effectively, thereby enhancing the plastic deformation of the material and decreasing the hardness[30]. Besides the decrease of mica phase, more forsterite appears in F3P7, which will also improve the hardness[31].

Figure 7 shows the fracture surface of the F5P5 glass-ceramics after mechanical property tests. The cleavage of mica phase can be observed in region A.

Compared with mechanical properties of other mica glass-ceramics[11], the transverse rupture strength in this work is a little bit lower, largely due to the residual porosity. However, considering the low sintering temperatures, the mica glass-ceramics can be more easily used for complex-shaped structures by powder metallurgy.

4. Conclusions

1) Mica glass-ceramics can be successfully prepared by using melting and powder metallurgy at low temperatures. The melting temperature of the glass-ceramics can be 1300 °C, which is 200 °C lower than that of conventional mica glass-ceramics.

2) For F3P7 and F4P6, the nepheline precipitates before mica between 662 and 694 °C. However, for F5P5, mica precipitates firstly as the main phase.

3) Bulk mica glass-ceramics can be obtained through sintering powder compacts at temperatures of 850 °C and 900 °C. The sintered density can be as high as 90%, and the microstructures are well crystallized, containing mainly mica and nepheline phases.

4) The transverse rupture strength and the hardness can be improved with the sintering temperature from 800 to 850 °C. High mechanical properties can be obtained in F3P7 samples sintered at 850 °C. The transverse rupture strength and the hardness are 93.02 MPa and 6.24 GPa, respectively. The mechanical properties are highly dependent on the sintered porosity and the phase constitutions.

Acknowledgement

This work was financially supported by the National Natural Science Foundation of China (No. 51272289 and 51504295) and the Open-End Fund for the Valuable and Precision Instruments of Central South University.

Reference

[1] D.G. Grossman, Machinable Glass-ceramics based on tetrasilicic mica, Journal of the American Ceramic Society 55 (9) (1972) 446-449.

[2] W. Holand, G.H. Beall, Glass-ceramic technology, John Wiley & Sons, 2012.

[3] W. Höland, W. Vogel, W. Mortier, P.-H. Duvigneaud, G. Naessens, E. Plumat, A new type of phlogopite crystal in machineable glass-ceramics, Glass technology 24 (6) (1983) 318-322.

[4] Y. Liu, X. Sheng, X. Dan, Q. Xiang, Preparation of mica/apatite glass-ceramics biomaterials, Materials Science and Engineering: C 26 (8) (2006) 1390-1394.

[5] Y. Liu, Q. Xiang, Y. Tan, X. Sheng, Nucleation and growth of needle-like fluorapatite crystals in bioactive glass-ceramics, Journal of Non-Crystalline Solids 354 (10) (2008) 938-944.

[6] T. Zaharescu, E. Nemeş, M. Râpa, E. Grosu, Radiation modification of functional properties in PVC/mica electrical insulations, Polymer Bulletin 57 (1) (2006) 83-90.

[7] W. Höland, P. Wange, K. Naumann, J. Vogel, G. Carl, C. Jana, W. Götz, Control of phase formation processes in glass-ceramics for medicine and technology, Journal of Non-Crystalline Solids 129 (1-3) (1991) 152-162.

[8] Q. Xiang, Y. Liu, X. Sheng, X. Dan, Preparation of mica-based glass-ceramics with needle-like fluorapatite, Dental Materials 23 (2) (2007) 251-258.

[9] T. Hamasaki, K. Eguchi, Y. Koyanagi, A. Matsumoto, T. Utsunomiya, K. Koba, Preparation and characterization of machinable mica glass-ceramics by the sol-gel

process, Journal of the American Ceramic Society 71 (12) (1988) 1120-1124.

[10] W.Y. Zhang, H. Gao, Fluorosilicate glass-ceramics : microstructure, fabrication and properties, Chemical Industry Press, Beijing,China, 2011.

[11] W.Y. Zhang, H. Gao, Microstructures, properties and fabrication of machinable ceramics [J], Journal of Synthetic Crystals 1 (2005).

[12] X.P. Ma, G.X. Li, L. Shen, Z.H. Jin, Ductile-mode material removal of a mica-glass-ceramic, Journal of the American Ceramic Society 86 (6) (2003) 1040-1042.

[13] X.M. Qin, Z.M. Xiu, L. Zuo, S. Li, Low melting temperature machinable bioactive glass-ceramics [J], Journal of Inorganic Materials 6 (2003) 001.

[14] X. Ma, G. Li, L. Shen, Microstructure and properties of a machinable glass-ceramic with low melting temperature, Wuji Cailiao Xuebao(Journal of Inorganic Materials)(China)(USA) 15 (2000) 265-370.

[15] M. Wei, Y. Zhang, X. Sun, L. Zhou, K. Wang, Low melting temperature machinable glass-ceramics, Key Engineering Materials 240-242 (2003) 241-244.

[16] T. Ooishi, A. Matsumoto, Production process for machinable ceramics, Patent NumberEP 0421391 (1991).

[17] H. Shao, T. Wang, Q. Zhang, Preparation and properties of CaO-SiO_2-B_2O_3 glass-ceramics at low temperature, Journal of Alloys and Compounds 484 (1) (2009) 2-5.

[18] E. Hamzawy, H. Darwish, Crystallization of sodium fluormica $Na(Mg,Zn,Ca)_{2.5}Si_4O_{10}F_2$ glasses, Materials chemistry and physics 71 (1) (2001) 70-75.

[19] K. Matusita, S. Sakka, Kinetic study of crystallization of glass by differential thermal analysis-criterion on application of Kissinger plot, Journal of Non-Crystalline Solids 38 (1980) 741-746.

[20] K. Cheng, J. Wan, K. Liang, Differential thermal analysis on the crystallization kinetics of K_2O-B_2O_3-MgO-Al_2O_3-SiO_2-TiO_2-F glass, Journal of the American Ceramic Society 82 (5) (1999) 1212-1216.

[21] P. Maiti, A. Mallik, A. Basumajumdar, P. Guha, Influence of barium oxide on the crystallization, microstructure and mechanical properties of potassium fluorophlogopite glass-ceramics, Ceramics International 38 (1) (2012) 251-258.

[22] A. Nassar, E. Hamzawy, F. Hafez, S. El Dera, C. Rüssel, Fluorphlopgopite ceramic via sintering of glass using inexpensive natural raw materials, Ceramics International 38 (3) (2012) 1921-1926.

[23] B.A. Rad, P. Alizadeh, Pressureless sintering and mechanical properties of SiO_2-Al_2O_3-MgO-K_2O-TiO_2-F(CaO-Na_2O) machinable glass-ceramics, Ceramics International 35 (7) (2009) 2775-2780.

[24] Z. Strnad, Glass-ceramic materials: liquid phase separation, nucleation and crystallization in glasses, Elsevier Science Publishers, P. O. Box 211, 1000 AE Amsterdam, The Netherlands, 1986. 268 (1986).

[25] K. Cheng, J. Wan, K. Liang, Hot-pressed mica glass-ceramics with high strength and toughness, Journal of the American Ceramic Society 82 (6) (1999) 1633-1634.

[26] P. Alizadeh, B.E. Yekta, T. Javadi, Sintering behavior and mechanical properties of the mica-diopside machinable glass-ceramics, Journal of the European Ceramic Society 28 (8) (2008) 1569-1573.

[27] M.I. Martín, F. Andreola, L. Barbieri, F. Bondioli, I. Lancellotti, J.M. Rincón, M. Romero, Crystallisation and microstructure of nepheline-forsterite glass-ceramics, Ceramics International 39 (3) (2013) 2955-2966.

[28] E. Bernardo, F. Andreola, L. Barbieri, I. Lancellotti, Sintered glass-ceramics and glass-ceramic matrix composites from CRT panel glass, Journal of the American Ceramic Society 88 (7) (2005) 1886-1891.

[29] M. Goswami, A. Sarkar, T. Mirza, V. Shrikhande, K. Gurumurthy, G. Kothiyal, Study of some thermal and mechanical properties of magnesium aluminium silicate glass-ceramics, Ceramics international 28 (6) (2002) 585-592.

[30] A.R. Molla, B. Basu, Microstructure, mechanical, and in vitro properties of mica glass-ceramics with varying fluorine content, Journal of Materials Science: Materials in Medicine 20 (4) (2009) 869-882.

[31] E. Hamzawy, Crystallization behaviour of fluorphlogopite glass-ceramics, Ceramics 45 (3) (2001) 89-96.

Table 1 Chemical compositions of the parent glass (wt.%) .

CaO	SiO_2	B_2O_3	Na_2O	MgO	ZnO
30%	25%	24%	7%	7%	7%

Table 2 Compositions of glass-ceramics in a mixture of parent glass and fluorphlogopite (wt.%).

	F3P7	F4P6	F5P5
Parent glass	30%	40%	50%
Fluorphlogopite	70%	60%	50%

Fig.1. XRD patterns of as quenched glasses containing mica.

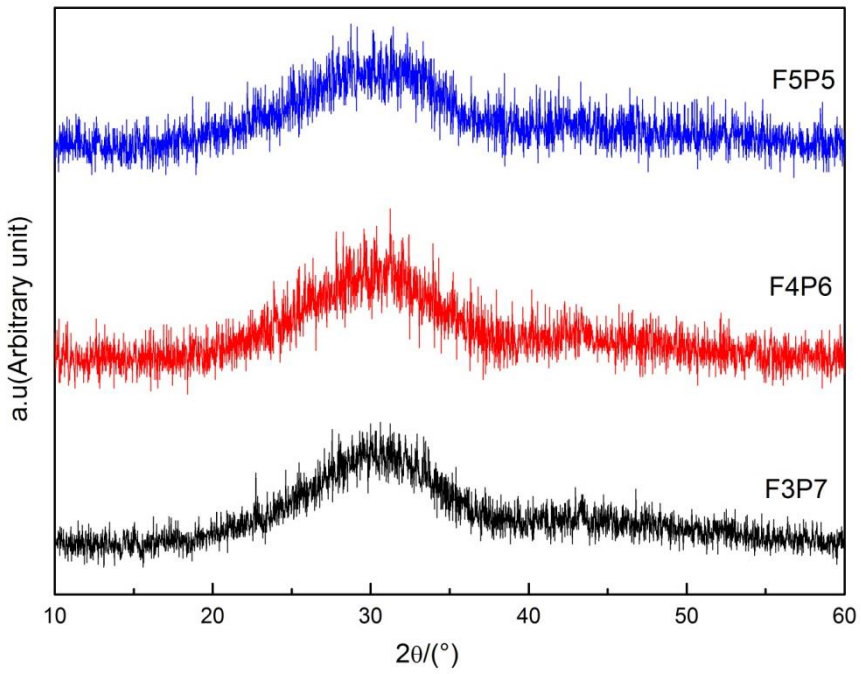

Fig.2. DSC curves of glass powders at different heating rates (a) F3P7, (b) F4P6 and (c) F5P5.

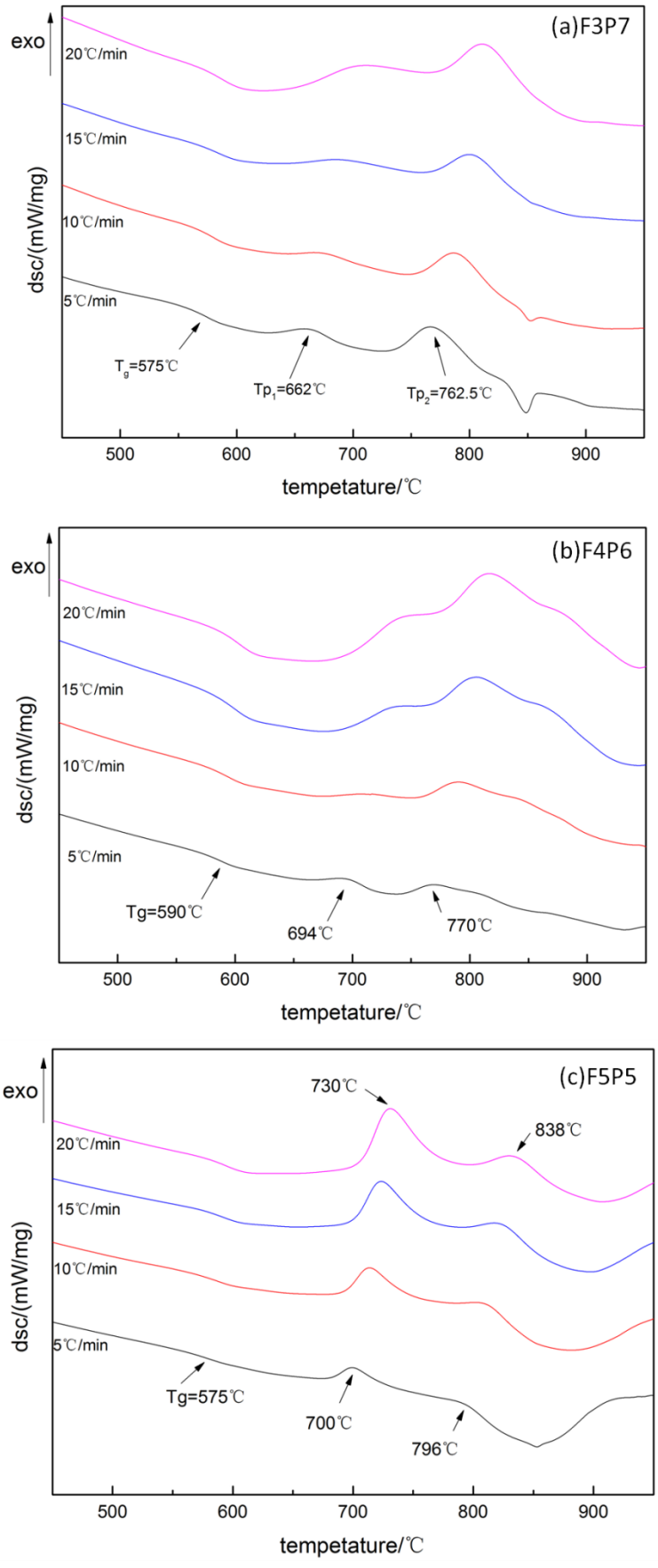

Table 3 Characteristic temperatures of T_g, T_{p1} and T_{p2} at varying heating rates.

	Heating reat (℃/min)	**T_g(℃)**	**T_{p1}(℃)**	**Activation energy E (kJ/mol) of T_{p1}**	**Δ T(℃) =T_{p1}-T_g**	**T_{p2}(℃)**	**Activation energy E (kJ/mol) of T_{p2}**
F3P3	5	575	662	107.9±13.1	87	762	133±3.3
	10	578	672		94	787	
	15	580	691		109	800	
	20	587	704		117	811	
F4P6	5	590	694	126.8±6.3	104	770	144.3±9.2
	10	592	707		115	789	
	15	600	735		135	804	
	20	604	743		139	816	
F5P5	5	570	700	176.3±12.5	125	796	169.6±21.6
	10	579	714		135	811	
	15	587	726		139	824	
	20	590	730		140	838	

Fig.3. Sintering shrinkage of the compacts at a heating rate of 5°C /min.

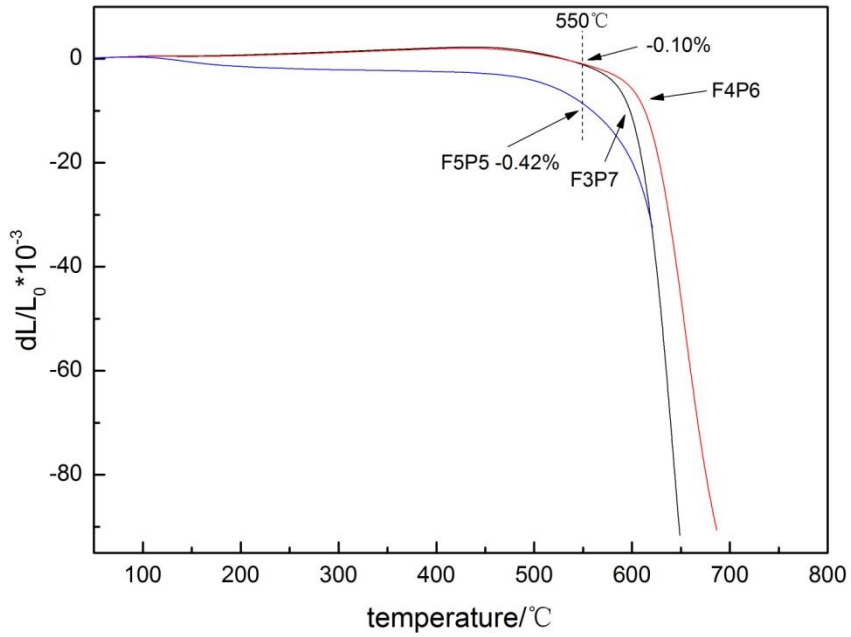

Fig.4. XRD patterns of glass-ceramics at different temperatures (a) F3P7, (b) F4P6 and (c) F5P5. [▲-mica, ●-nepheline, △-cordierite, ★- forsterite, ■-augite].

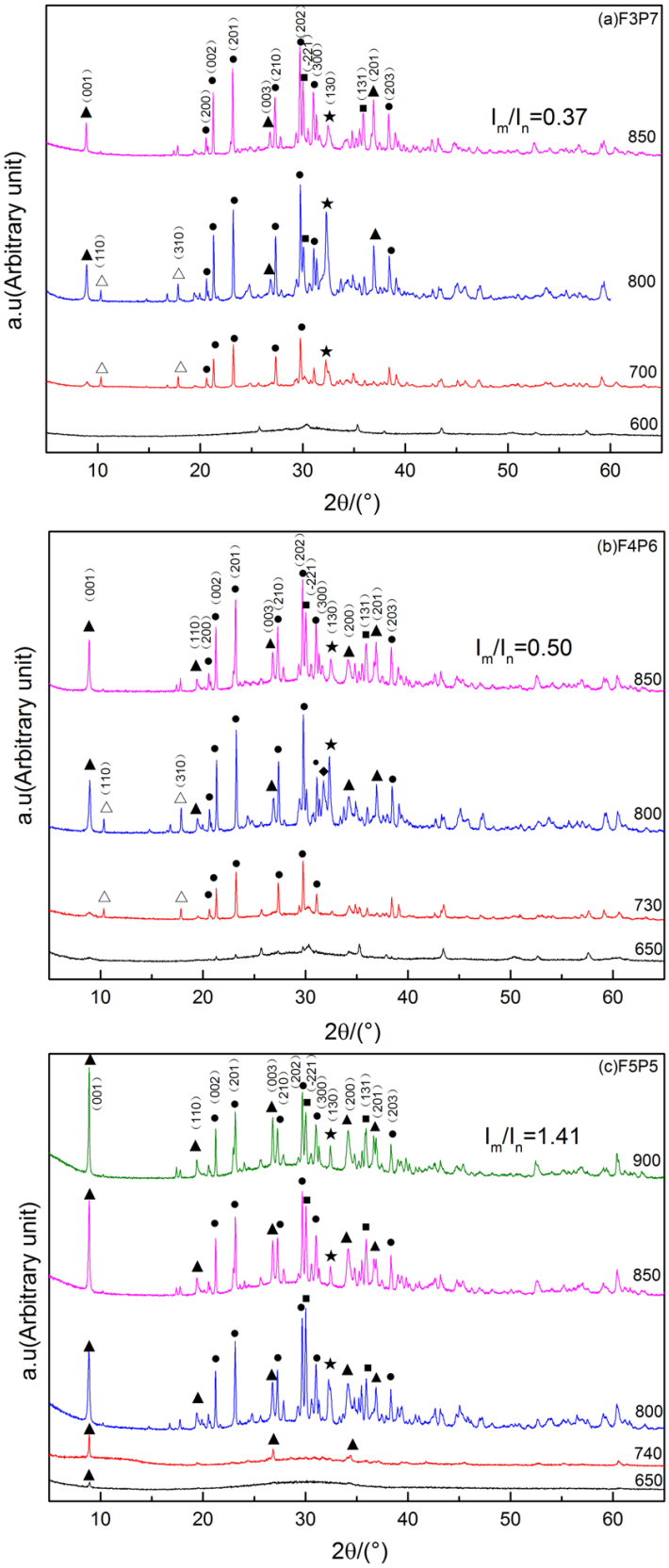

Fig.5. SEM images of F3P7 sintered at (a) 800°C, (b) 850°C and F4P6 at (c) 800°C, (d) 850°C. The flake-like mica of (a), (b), (c) and (d) were marked by arrows.

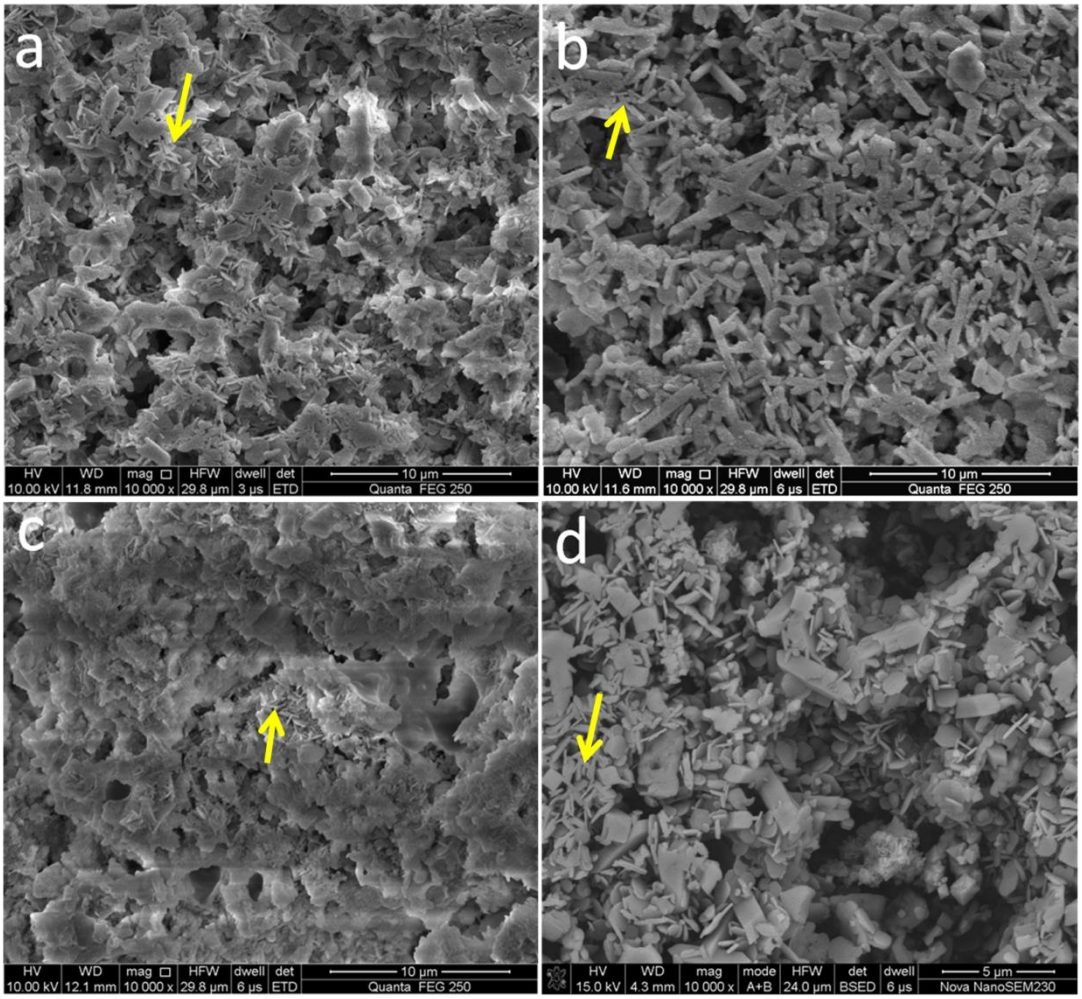

Fig.6. SEM images of F5P5 sintered at (a) 800°C, (b) 850°C and (c) 900°C. The higher magnification (×4 0000) of (a) is in (a1) and the flake-like mica of (a), (b) and (c) were marked by arrows.

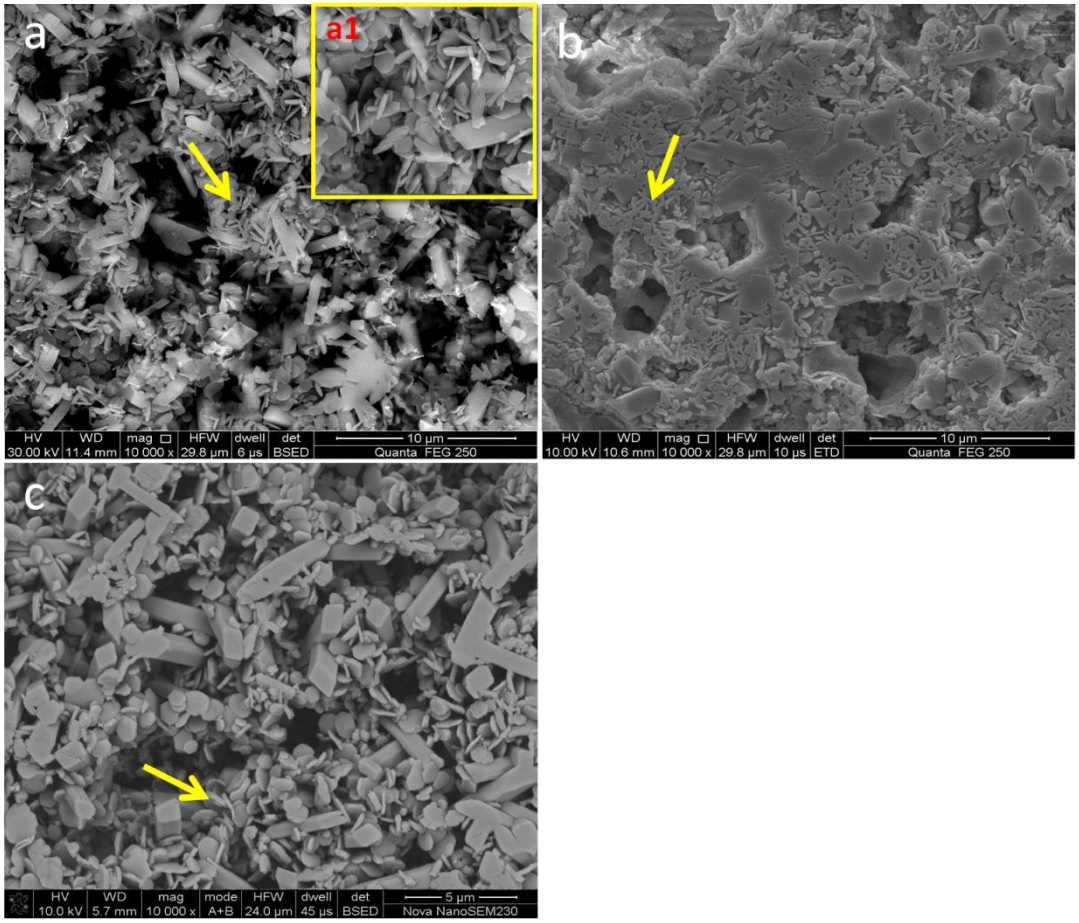

Fig.7. The fractograph of F5P5 sintered at 850°C.

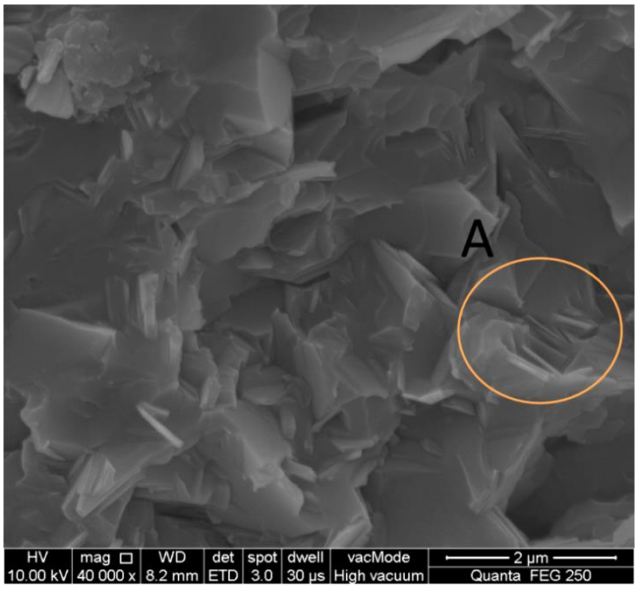

Table 4 The density and mechanical properties of mica glass-ceramics.

		Density (g/cm^3)	Aspect ratio	Bending strength(MPa)	Hardness（200g）	Porosity
F3P7	800℃	2.50±0.2	6.3	37.42±15.1	120±36	>15%
	850℃	2.70±0.2	5.0	93.02±17.9	624±89	12%
F4P6	800℃	2.42±0.1	8.2	54.52±11.4	82±45	>15%
	850℃	2.79±0.3	5.9	89.96±5.2	539±101	9.5%
F5P5	800℃	2.27±0.2	9.0	33.52±10.5	61±44	>15%
	850℃	2.65±0.2	6.8	48.88±7.7	411±119	14.4%
	900℃	2.75±0.1	5.4	78.02±6.2	403±110	9.7%